SWIFT-UVOT-CALDB-##
Date Original Submitted: 7th November 2005
Prepared by: Tracey Poole
Date Revised:
Revision #01
Revised by:
Pages Changed:
Comments:

SWIFT UVOT CALDB RELEASE NOTE

SWIFT-UVOT-CALDB-##: Effective Area Curves

0. Summary:

This product provides the in-orbit effective area curves for the 7 filters of the UVOT.

1. Component Files:

FILE NAME	VALID DATE	RELEASE DATE	VERSION

2. Scope of Document:

This document contains a description of the effective area curve calibration analysis performed to produce the effective area curve calibration products for the UVOT calibration database.

3. Changes:

This is the first release of the in-orbit effective area curves, replacing ground based calibration data.

4. Reason For Update:

An update was undertaken to improve the effective area curve calibration with in-orbit observations of known standard stars.

5. Expected Updates:

Further updates are expected following further analysis of PSF and coincidence loss correction.

6. Caveat Emptor:

The original ground-based effective area curves (SWIFT UVOTA calibration files: 20041116) were calculated incorrectly, therefore a comparison between these in-orbit curves and the ground-based curves in earlier versions of the CALDB is meaningless.

Due to the lack of faint spectroscopic standard stars, especially in the ultraviolet, the effective area curves have been calibrated with very few stars.

7. Data Used:

Observations of 4 white dwarfs and 2 Oke standard stars were taken in the UVOT filters. Where multiple observations were taken, images were spatially corrected and then co-added. Observation details, sorted by observation date, can be seen in Table 1.

Object Name	Filter	Date	ID	Mode	Exposure Time (sec)
WD1657+343	uvm2	25/02/2005	55900001	E	707.01
WD1657+344	uvw1	25/02/2005	55900002	E	572.35
WD1657+343	uvw2	25/02/2005	55900001	E	740.79
WD1657+343	v	25/02/2005	55900002	E	605.79
WD1121+145	uvm2	04/03/2005	55250010	E	671.82
WD1121+145	uvw1	04/03/2005	55250011	E	139.61
WD1121+145	uvw2	04/03/2005	55250010	E	715.78
WD1121+145	v	04/03/2005	55250011	E	412.77
WD1121+145	uvm2	05/03/2005	55250015	E	753.42
WD1121+145	uvm2	05/03/2005	55250015	I	760.102

WD1121+145	uvw1	05/03/2005	55250017	E	693.81
WD1121+145	uvw1	05/03/2005	55250017	I	699.719
WD1121+145	uvw2	05/03/2005	55250013	E	753.08
WD1121+145	uvw2	05/03/2005	55250013	I	759.694
WD1657+343	uvm2	06/03/2005	55900018	E	693.04
WD1657+343	uvm2	06/03/2005	55900018	I	698.704
WD1657+344	uvw1	06/03/2005	55900020	E	573.43
WD1657+344	uvw1	06/03/2005	55900020	I	580.012
WD1657+343	uvw2	06/03/2005	55900016	E	693.44
WD1657+343	uvw2	06/03/2005	55900016	I	700.201
WD1121+145	b	05/04/2005	55250019	I	1045.97
WD1657+343	u	12/04/2005	55900024	I	643.959
WD1657+343	v	12/04/2005	55900025	I	640.45
WD1121+145	v	13/04/2005	55250020	I	1577.75
WD1121+145	white	10/05/2005	55250021	I	54.1386
WD1657+343	uvw2	19/06/2005	55900029	I	685.464
WD1657+343	b	20/06/2005	55900030	I	951.898
WD1121+145	u	20/06/2005	55250023	I	487.445
WD1657+343	white	25/06/2005	55900032	I	157.362
WD1026+453	b	07/07/2005	55761006	I	455.297
sa95-42	b	07/07/2005	55763001	I	568.482
sa95-42	b	07/07/2005	55763003	I	569.409
WD0947+857	b	07/07/2005	55760005	I	395.554
G24-9	b	07/07/2005	55762002	I	655.488
WD1026+453	u	07/07/2005	55761005	I	290.699
WD0947+857	u	07/07/2005	55760004	I	236.541
WD1026+453	uvm2	07/07/2005	55761004	E	400.709
WD0947+857	uvm2	07/07/2005	55760002	E	400.709
WD0947+857	uvw1	07/07/2005	55760003	E	236.541
sa95-42	v	07/07/2005	55763002	I	509.655
sa95-42	v	07/07/2005	55763004	I	509.004
G24-9	v	07/07/2005	55762001	I	1032.82

Table 1 – Table containing the observations used to calculate the in-orbit zero points. All of the sequence numbers in column 4 are missing their first three digits of 000. In column 5, I represents Image mode, and E represents Event mode

8. Description of Analysis:

The first step to calculating the in-orbit effective area curves was to correct the ground-based effective area curves. The in-orbit effective area curves were then calculated using in-orbit data analysis to update the new ground-based effective area curves.

8.1. Ground-Based Effective Area Curves

A smooth white filter effective area curve was created using a spline fit to the 6 ground-based filter points given in Table2. This smooth white filter curve is plotted in yellow in Figure 3.

Filter	Wavelength (Å)	Effective Area (cm^2)
UVW1	1930.0	86.26
UVM2	2200.0	98.73
UVW1	2600.0	106.73
U	3450.0	80.29
B	4370.0	47.17
V	5480.0	26.03

Table 2 - Ground-based calibration points.

The optical and UV filter ground-based effective area curves were calculated using the respective transmission filter curves seen in Figure 2. These transmission curves were then convolved with the white filter effective area curve (assuming that the white filter is transparent) to produce the ground-based effective area curves shown in Figure 3.

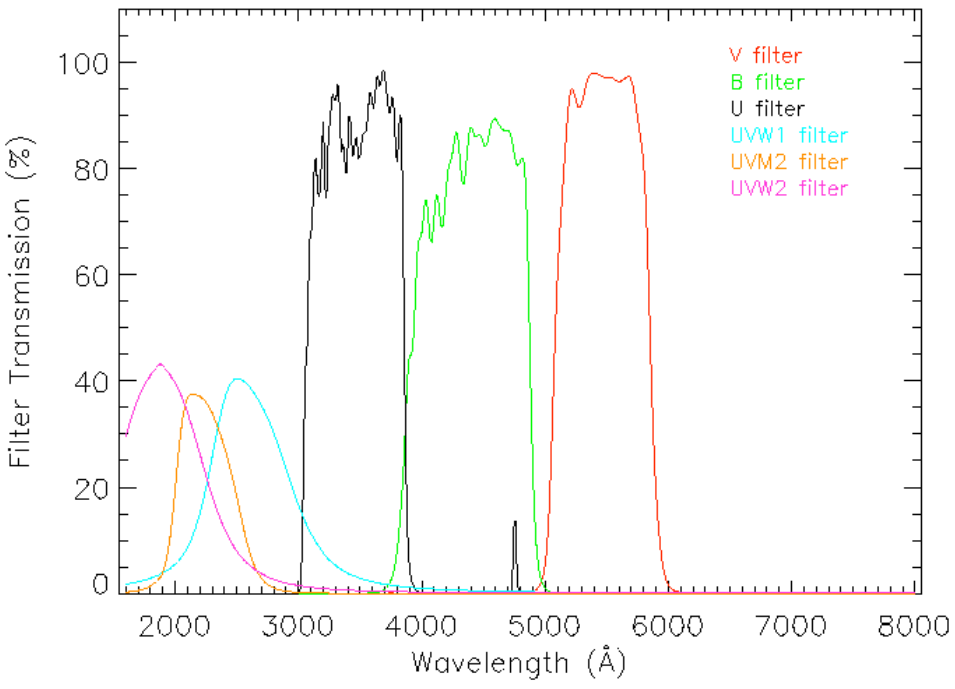

Figure 1 - Filter transmission curves.

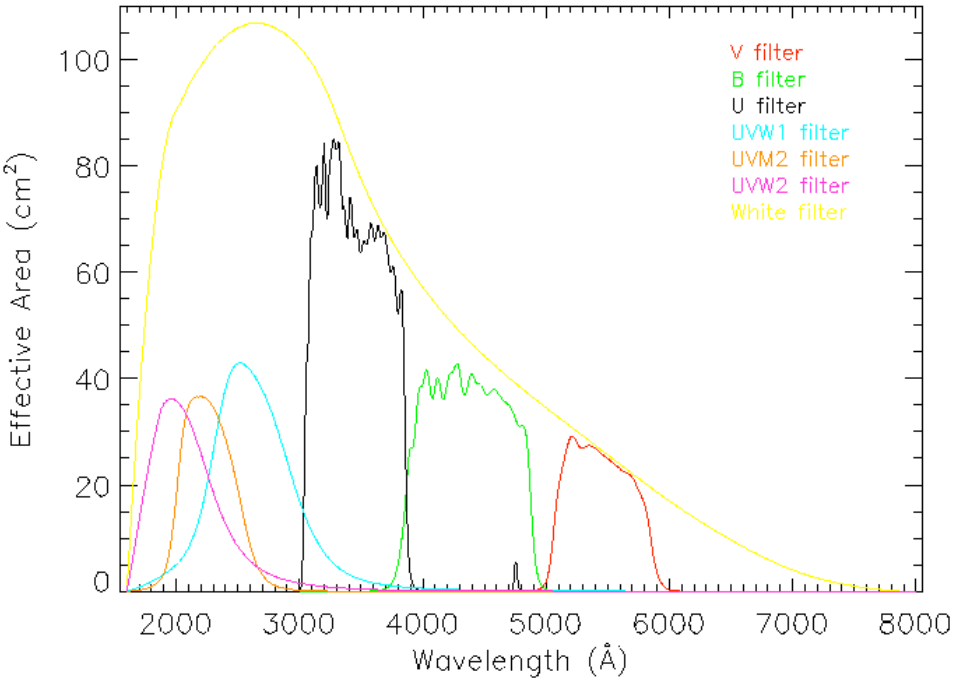

Figure 2 - Ground-based effective area curves.

Two methods were used to calculate the in-orbit effective area curves; one using count rate analysis, the other using zero point analysis. Due to the uncertainty of the ground based zero points, the in-orbit effective area curves were created using the count rate ratio method.

8.2. In-Orbit Effective Area curves

Observations of 4 white dwarfs and 2 Oke standard stars were taken in the UVOT filters (see Table 1 for details). Where multiple observations were taken, images were spatially corrected and then co-added. All observations were reprocessed using the latest CALDB teldef file (swugen20041120v102.teldef). The observed count rate was obtained using a 12 pixel (6 arcsec) aperture radius for optical filters and a 24 pixel (12 arcsec) radius for ultraviolet filters. All observed count rates were then corrected using the theoretical coincidence loss equation,

$$C_{theory} = \frac{-\ln(1 - C_{raw} ft)}{ft(1 - df)},$$

Where C_{theory} is the theoretically coincidence loss corrected count rate, C_{raw} is the raw observed count rate, ft is the frame time (0.011088s), and df is the deadtime fraction (0.0155844). This theoretical coincidence loss is then corrected by multiplying by the ground-based empirical formula,

$$f(x) = 1.0 + 0.2966x - 0.492x^2 - 0.4183x^3 + 0.2668x^4,$$

Where $x = C_{raw} ft$.

The expected count rates of the 6 observed stars in each filter were obtained by convolving the known spectrum of each source with the new ground based effective area curves. The spectra of WD1657+343, WD0947+867 and WD1026+453 had to be extrapolated beyond 5700Å which will affect the V filter. The spectrum of WD1121+145 was complete across the wavelength range 1600-8000Å. The spectra of SA95-42 and G24-9 range from 3200-8000Å, which will affect all the UV filters and the U filter.

Tables 3 shows the results using these 6 observed stars, where C_{raw} is the raw observed count rate, T_{exp} is the total exposure time of the observation, C_{obs} is the coincidence loss corrected count rate, C_{exp} is the simulated count rate, and C_{ratio} is the ratio of observed to simulated count rates (C_{obs}/C_{exp}).

Source	Filter	T_{exp} (s)	C_{raw} (ph/s)	C_{obs} (ph/s)	C_{exp} (ph/s)	C_{ratio} (ph/s)
WD1657+343	V	1246	3.56±0.07	3.74±0.07	4.88	0.77
WD1657+343	B	952	13.11±0.14	14.85±0.16	17.61	0.84
WD1657+343	U	644	26.19±0.26	32.57±0.30	47.55	0.68
WD1657+343	UVW1	1726	30.37±0.14	38.80±0.21	60.87	0.64
WD1657+343	UVM2	2099	25.70±0.11	31.86±0.16	49.71	0.64
WD1657+343	UVW2	1426	44.30±0.18	61.47±0.36	71.07	0.86
WD0947+867	B	396	24.51±0.32	27.55±0.37	33.88	0.81
WD0947+867	U	237	49.24±0.50	58.93±0.65	89.71	0.66
WD0947+867	UVW1	237	57.61±0.51	70.34±0.71	109.81	0.66
WD0947+867	UVM2	401	48.05±0.35	57.34±0.46	88.45	0.65
WD1026+453	B	455	17.46±0.25	19.26±0.29	24.79	0.78
WD1026+453	U	291	34.05±0.37	39.23±0.45	62.45	0.63
WD1026+453	UVM2	401	47.84±0.35	57.07±0.46	58.32	0.98
WD1121+145	V	2678	2.87±0.05	2.99±0.05	3.36	0.89

WD1121+145	B	1046	11.13±0.13	12.41±0.15	12.08	1.03
WD1121+145	U	487	21.07±0.23	25.30±0.31	36.81	0.68
WD1121+145	UVW1	1533	25.88±0.14	32.12±0.19	49.06	0.65
WD1121+145	UVM2	2185	21.50±0.10	25.89±0.13	40.77	0.88
WD1121+145	UVW2	2229	36.04±0.13	47.68±0.22	56.22	0.85
SA95-42	V	1019	7.54±0.13	8.16±0.14	11.16	0.73
SA95-42	B	1138	24.05±0.18	29.48±0.26	36.24	0.81
G24-9	V	1033	6.95±0.10	7.49±0.16	9.30	0.80
G24-9	B	655	13.85±0.17	15.77±0.22	17.90	0.88

Table 3 - Count Rate results for WD1657+343, WD0947+867, WD1026+453, WD1121+145, SA95-42 and G24-9.

8.3. Comparing the Ratio Results

The average ratios can be seen in Table 4, along with the ratio results for WD1657+343, WD0947+867, WD1026+453, WD1121+145, SA95-42 and G24-9.

Filter	Count Rate Ratio WD1657 +343	Count Rate Ratio WD0947 +867	Count Rate Ratio WD1026 +453	Count Rate Ratio WD1121 +145	Count Rate Ratio Sa95-42	Count Rate Ratio G24-9	Aver. Ratio
V	0.77	-	-	0.89	0.73	0.80	0.80±0.07
B	0.84	0.81	0.78	1.03	0.81	0.88	0.86±0.09
U	0.68	0.66	0.63	0.68	-	-	0.66±0.02
UVW1	0.64	0.64	-	0.65	-	-	0.64±0.01
UVM2	0.64	0.65	0.98	0.88	-	-	0.77±0.17
UVW2	0.86	-	-	0.85	-	-	0.86±0.01

Table 4 - Ratio results used to produce the in-orbit effective are curves.

Figure 4 shows the comparison between the in-orbit effective area curves using the average count rate ratios (solid lines), and the ground based effective area curves (dashed lines).

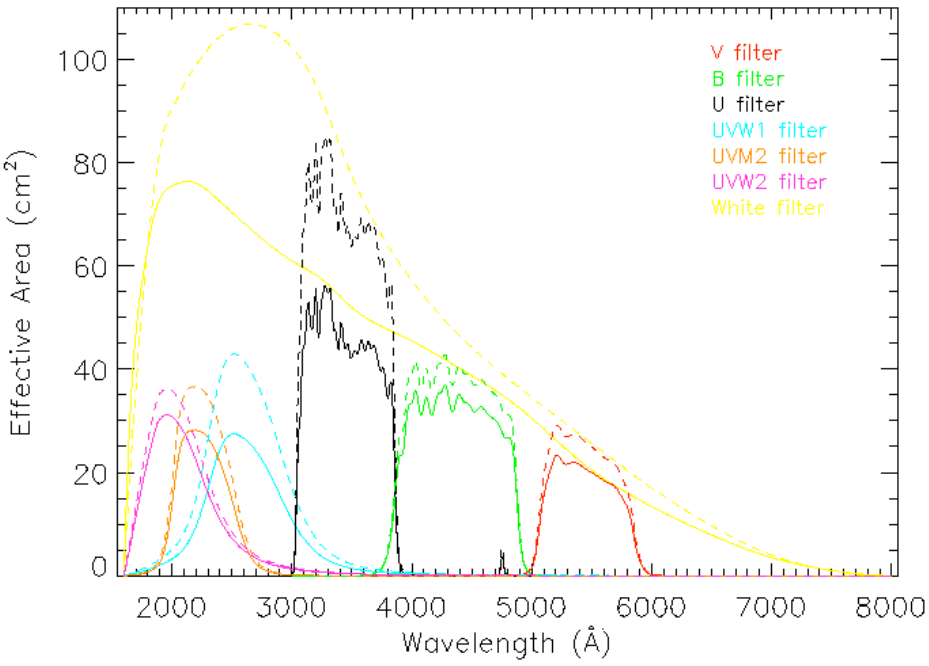

Figure 3 - Effective area curves using the average count rate ratio. Solid lines are in-orbit curves, dashed lines are ground-based curves.

8.4. Predicted Effective Area Curves

Predicted effective area curves were created by considering the known responses of the UVOT detector and filters in the wavelength region 1600Å to 8000Å. The following were considered when calculating the predicted effective area curves:-

1. Transmission curves for each filter
2. Quantum efficiency of the photon counting system (D.Q.E)
3. Mirror reflectivity
4. Telescope area (596cm^2)

Figure 6 shows the predicted effective area curves produced by convolving these sub-component measurements using,

$$EffectiveAreaCurve = Transmission \times DQE \times MirrorReflectivity^3 \times 596,$$

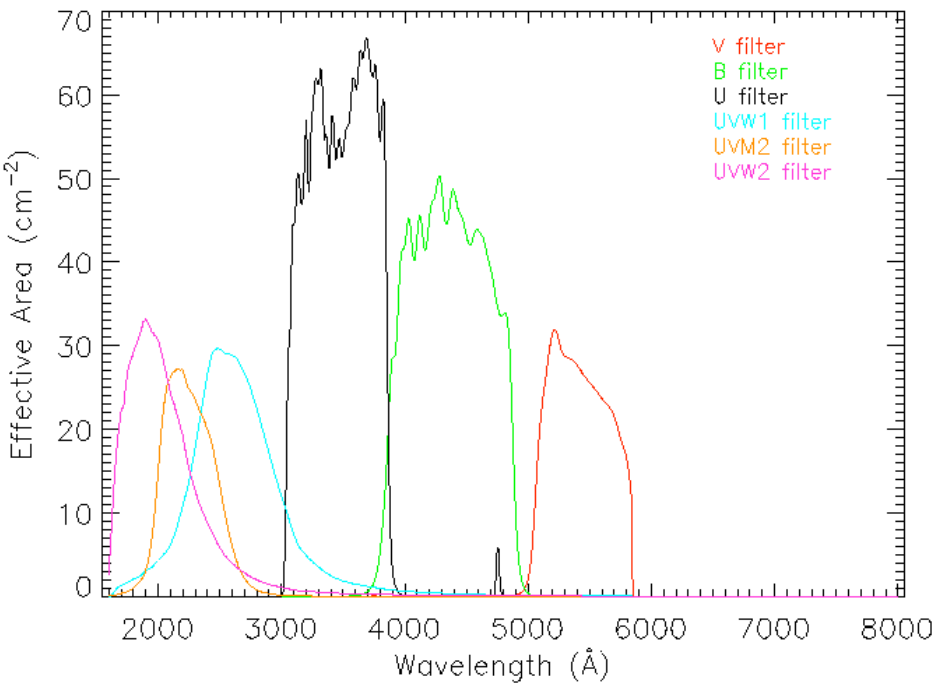

Figure 4 - Predicted effective area curve for UVOT.

8.5. Comparing the different Effective Area Curves

Table 5 shows the ratios of in-orbit to ground (Column 2), ground to predicted (Column 3), and in-orbit to predicted (Column 4) ratios. Errors in the ground-based measurements and instrument responses are not taken into account here, but will add uncertainty to these results (the error in the D.Q.E. measurement is up to 10%). The plots of these comparisons can be seen in Figures 3, 5 and 6 respectively.

Filter	In-Orbit/Ground	Ground/Predicted	In-Orbit/Predicted
V	0.80±0.07	0.99	0.79
B	0.86±0.09	0.88	0.76
U	0.66±0.02	1.22	0.80
UVW1	0.64±0.01	1.34	0.89
UVM2	0.77±0.17	1.37	1.05
UVW2	0.86±0.01	1.14	0.97

Table 5 - Ratio results when comparing predicted, in-orbit and ground-based effective area curves.

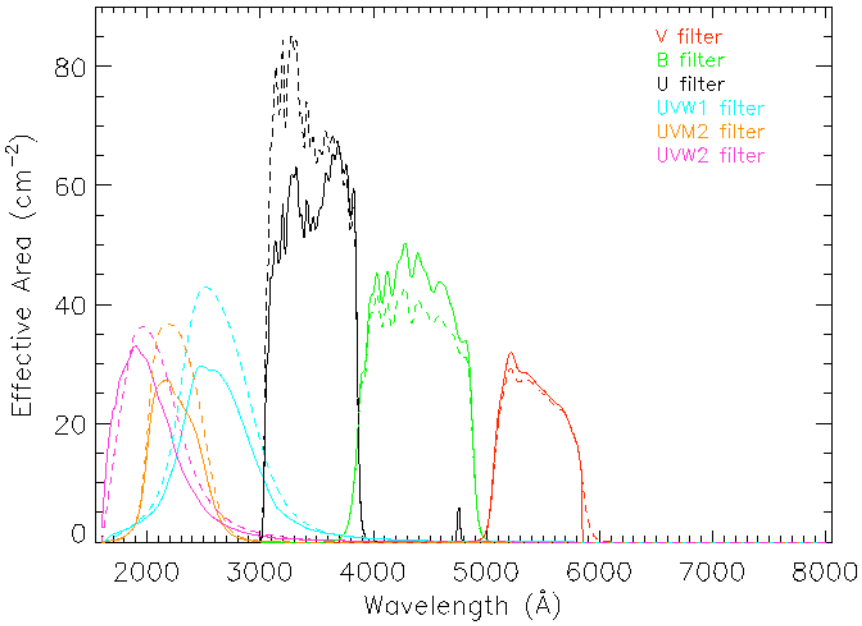

Figure 5 - Comparison of predicted effective area curves (solid lines) to ground-based effective area curves (dashed lines).

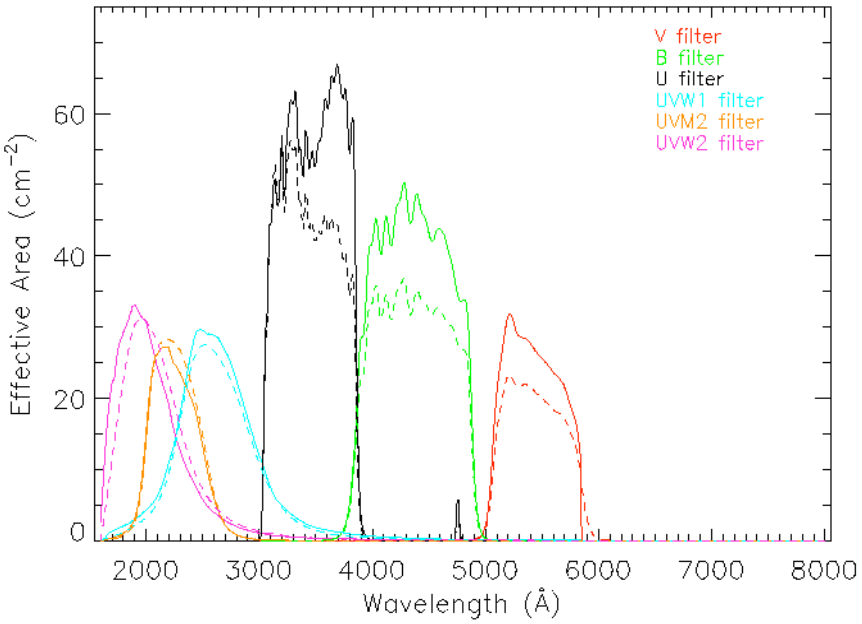

Figure 6 - Comparison of predicted effective area curves (solid lines) to in-orbit effective area curves (dashed lines).

Figure 5 and Table 5 show that in the case of the ultraviolet and the U filters, the ground-based effective area curves are higher than expected from the predicted data. This suggests there may either be a problem with the ground-based calibration, or there is something missing in the predicted data. Figure 5 also shows that the V filter ground-based calibration agrees with the predicted, but there is a decrease in the B filter ground-based calibration compared to the predicted results.

Figure 6 and Table 5 show that in general, the in-orbit effective area curves have decreased when comparing to the predicted curves. The optical filters show a greater decrease than the UV filters. We also see this larger decrease in the optical when comparing the ground-based and in-orbit zero points.